Extracting the Critical Points of Formaldehyde (HCHO) Emission Model in Hot Desert Climate

Air, Soil and Water Research
Volume 15: 1–15

DOI: 10.1177/11786221221105082

Chuloh Jung and Naglaa Sami Abdelaziz Mahmoud

College of Architecture, Art and Design, Healthy and Sustainable Built Environment Research Center, Ajman University, United Arab Emirates.

ABSTRACT: Indoor air pollutants have various emission patterns and are influenced by indoor microclimate, the physical properties of building materials, and types of chemical substances. The difference in these emission patterns affects the prediction via simulation. This paper aims to extract factors that have an important influence on selecting empirical models by examining the emission pattern of formaldehyde (HCHO) from building materials. As a methodology, Small Chamber Pollutant Emission Test was used for six different flooring and wallpaper specimens, and HCHO was sampled and analyzed using HPLC (High-Performance Liquid Chromatography). The result showed that the higher the linear relationship between emission intensity and time, the more appropriate the first-order reduction model, such as flooring-A (R^2 = .99), flooring-B (R^2 = .94), wallpaper-A (R^2 = .99), and wallpaper-C (R^2 = .98). The emission pattern of HCHO in building materials is classified into three types: In type I (R^2 = .00–.11), the emission of chemical substances reaches the maximum after the start of the experiment and decreases relatively rapidly. Type II (R^2 = .00–.41), the emission pattern having the shape of a vertex with a refined concentration ascending and a gentle descending and is a type in which the suitability is significantly high in the concentration descending section, and Type III (R^2 = .33–.60), which shows a mild linear increase and decreases trend in the ascending and concentration dropping sections. It is a type that indicates the suitability with the predicted value in a meaningful way in the entire area. Even though many previous studies focused on the concentration descending section in different materials (R^2 = .51–.95), it was confirmed that the emission characteristics in the initial concentration ascending section are also critical points for simulation model selection since R^2 of ascending section of Type II (.67–.70) and Type III (.77–.93) turned out statistically meaningful except Type I (.02–.25).

KEYWORDS: Formaldehyde (HCHO), emission pattern, first order decay, double exponential decay, important factors, hot desert climate

TYPE: Original Research

CORRESPONDING AUTHOR: Chuloh Jung, Department of Architecture, College of Architecture, Art and Design, Healthy and Sustainable Built Environment Research Center, Ajman University, Al Jurf 1, P.O.Box 346, United Arab Emirates. Email: c.jung@ajman.ac.ae

Introduction

The generation of indoor air pollutants in building materials is influenced by many factors such as indoor microclimate, the physical properties of building materials and types of chemical substances, and the external environment. It has a variety of emission patterns (Awad & Jung, 2021; D'Ovidio et al., 2021; Jung & Awad, 2021; Kubečková et al., 2020). The emission pattern refers to the tendency to change due to the increase and decrease of chemical substances' emissions in the building material (Peng et al., 2017; Piasecki et al., 2018). This pattern has various shapes due to the difference in the initial emission amount, the maximum emission amount, the time to reach the peak, and the decreasing tendency (Liang & Yang, 2013). The difference in these emission patterns affects the prediction through simulation (Xing et al., 2020).

The use of simulation to predict chemical concentration is beneficial in saving time and money. It has meaning when the prediction through simulation becomes more consistent with the actual value (Palmisani et al., 2020; Rosen & Kishawy, 2012). The prediction of chemical substances is based on numerical and empirical models, and empirical models using measured values are beneficial based on their convenience (Cho & Choi, 2014; Peng et al., 2017). However, in the case of the practical model, only limited parameters are substituted, so it has limitations in predicting based on the diversity of the emission pattern (Breen et al., 2014).

Several previous researchers have reported the applicability of different empirical models based on the emission characteristics of various building materials such as paints, adhesives, and wood (Böhm et al., 2012; Kozicki & Guzik, 2021; Tudor et al., 2020; Wi et al., 2020). However, this has the aspect that there is a difference in the emission pattern depending on the content of chemical substances inside the building material (Khoshnava et al., 2020). Selecting the first order and double exponential decay models according to the type of building material involves risks in choosing an appropriate model (Gładyszewska-Fiedoruk et al., 2019; Huang et al., 2016). Therefore, it will be beneficial to extract and utilize factors for selecting a suitable empirical model based on the emission pattern that exists according to the characteristics of the material rather than the classification by the type of building material (Marzocca et al., 2017; Tran et al., 2020).

When estimating the emission intensity or indoor concentration of chemical substances, a numerical model based on the mass transfer equation and an empirical model based on actual values (Piasecki & Kostyrko, 2020). The more easily applicable is the practical model (Ahn et al., 2017). The first-order reduction models and the double exponential decay model (He et al.,

2019; Liu et al., 2015). The first-order decay model, proposed by Gunschera et al. (2013), is suitable for explaining the emission characteristics of chemical substances in which the evaporation process is dominant in building materials (equation (1)).

$$E(t) = E_0 \times e^{-k \cdot t} \quad (1)$$

$E(t)$ = Amount generated per unit area at time t (mg/m^{2}h)
E_0 = Amount generated per unit area at $t = 0$ (mg/m^{2}h)
k = first-order reduction constant (h^{-1})
t = time (h)

The double exponential decay model, proposed by de Gennaro et al. (2015), explains the emission characteristics of building materials in which internal emission is dominant (equation (2)).

$$E(t) = E_1 \times e^{-k_1 \cdot t} + E_2 \times e^{-k_2 \cdot t} \quad (2)$$

E_1 = Amount of occurrence at $t = 0$ in a rapidly decreasing process (mg/m^{2}h)
k_1 = Decrease constant for rapid decay (h^{-1})
E_2 = The amount of occurrence at $t = 0$ in a slow-decreasing process (mg/m^{2}h)
K_2 = Decrease constant for slow decay (h^{-1})
t = time (h)

The above empirical model equation was made based on the characteristics of the decreasing period rather than the application to the initial period of increasing concentration (Mocho et al., 2017).

Conformity verification by empirical models has been reported by many researchers (Ai et al., 2015; Jomehzadeh et al., 2017). They apply the model formula based on building materials, mainly considered diffusion-dominated and evaporation-dominated by the characteristics of the reduction section in the concentration change over time (Geng et al., 2017). Missia et al. (2010) reported that hazardous chemical substances were measured through small chamber experiments on wood and carpet, such as PB and plywood. As a result of prediction through a double exponential decay model, it showed high suitability in all materials. Salem et al. (2012) reported a higher fit in the double exponential decay model than the first-order reduction model due to predicting the HCHO concentration in new houses using measured data from PB and MDF. The above studies report the suitability of the double exponential decay model using wood products (Xiong et al., 2019). In applying the empirical model, the emission characteristics of the concentration ascending section are not considered, and the features of the emission intensity descending area after the maximum emission intensity are identified (Liu et al., 2015).

Wang et al. (2021) showed a difference in the initial emission amount and different radiation patterns. It was reported that the emission pattern of the specimen with a low initial emission amount, even though it was a wood product, was slightly reduced or showed an equilibrium state, indicating that the first-order reduction model was highly suitable (Hérault et al., 2010). It was also reported that even in the case of the same wood products, there was a difference in the emission pattern due to the difference in the initial emission amount, and there was a difference in the suitability of the model applied to it (Böhm et al., 2012).

Previous studies have reported a critical point in selecting an empirical model based on the emission pattern, and it is essential to determine an appropriate practical model based on this (Mu et al., 2020). It is judged that it will be helpful to increase the suitability of the model application to find factors that have an important influence on the model decision by further subdividing the emission pattern (Nogueira et al., 2017).

This study aims to derive factors that influence selecting empirical models, such as the primary reduction model and the double exponential decay model, by examining the emission pattern of formaldehyde (HCHO) emitted from building materials.

Materials and Methods

Construction materials overview

The building materials used in this study were the flooring and wallpaper used the most as interior finishing materials (Arar & Jung, 2021; Jung et al., 2021). Table 1 is an overview of experimental building materials. On the premise that the emission pattern differs depending on the chemical substances' content, different production dates were selected, or the number of elapsed days was selected differently by other testing dates for the same material (Sarbu & Sebarchievici, 2013).

Flooring-A and flooring-B are from the same manufacturer, while flooring-C is from a different manufacturer. Wallpaper-A and wallpaper-B are also from the same manufacturer, but wallpaper-C is from another manufacturer.

As for the storage form after the production of the above materials, the wallpaper was sealed in plastic, the flooring was packaged in a general paper box, and the materials stored at room temperature in the material warehouse of each producer were used.

Small chamber pollutant emission test

According to ISO (2020) (the International Organization for Standardization) a small chamber system 16,000, test pieces are prepared with 160 mm × 160 mm to analyze each specimen's hazardous chemical generation. HCHO was collected using an LpDNPH S10L cartridge (Supelco Inc., U.S) to contain carbonyl compounds (Williams et al., 2019). To remove the interference caused by Ozone (O_3), the O_3 scrubber was connected in front of the LpDNPH S10L cartridge, and the sample was collected by clicking it on a flow sampling pump (Tucker, 2014). At this time, 7.01 of collected air in the chamber was collected at 167 ml/min, and the collected samples

Table 1. Outline of Test Pieces.

CLASSIFICATION	MANUFACTURER	TEST PIECE SIZE	PRODUCTION DATE	EXPERIMENT DATE	DAYS PASSED
Flooring-A	Itlas (Italy)	160 mm × 160 mm	10/02/2021	19/03/2021	38
Flooring-B	Itlas (Italy)	160 mm × 160 mm	10/02/2021	16/05/2021	96
Flooring-C	Meister (Germany)	160 mm × 160 mm	02/09/2019	16/12/2020	456
Wallpaper-A	Arte (Belgium)	160 mm × 160 mm	28/02/2021	20/03/2021	20
Wallpaper-B	Arte (Belgium)	160 mm × 160 mm	28/02/2021	17/05/2021	78
Wallpaper-C	Casadeco (France)	160 mm × 160 mm	11/02/2019	03/12/2020	656

Table 2. Parameters for Prediction for Each Specimen.

CLASSIFICATION	INITIAL EMISSION INTENSITY (Mg/m²h)	DOUBLE EXPONENTIAL DECAY MODEL		FIRST-ORDER DECAY MODEL
		FIRST DECAY CONSTANT (h^{-1})	SECOND DECAY CONSTANT (h^{-1})	DECAY CONSTANT (h^{-1})
Flooring-A	1.30	0.00972	0.00146	0.00186
Flooring-B	8.42	0.00371	0.00122	0.00248
Flooring-C	9.80	0.00042	0.00186	0.00134
Wallpaper-A	1.36	0.01812	0.00278	0.00332
Wallpaper-B	1.48	0.00156	0.00062	0.00106
Wallpaper-C	0.74	0.01118	0.00064	0.00418

were stored in a cool and dark place until extraction (Even et al., 2021). For the extraction of the analytical model, the DNPH-carbonyl derivative formed by reacting with DNPH was extracted with 5 ml of HPLC grade acetonitrile, and analysis was performed immediately (Zhang et al., 2014). The examination for HCHO was performed using HPLC (High-Performance Liquid Chromatography, Shimadzu).

Since the UAE is located in a hot arid desert and the residents spend 90% of their time indoors with air-conditioning due to scorching summer and no apparent differences between seasons, The environmental conditions in the chamber were maintained at a temperature of 25°C, relative humidity of 50%. The number of ventilation at 0.5 times/h to simulate the indoor condition with central air-condition in Dubai, UAE. The sample loading rate was 2.2 m^2/m^3, the exposed surface area of the test piece was 0.044 m^2, and the emission intensity was calculated as shown in equation (3) below (Murata et al., 2013).

$$SER_a = \frac{C_t \times Q}{A} = \frac{C_t \times nV}{A} = C_t \times \frac{n}{L} = C_t \times q \quad (3)$$

SER_a = Emission amount per unit area of specimen (mg/m^2h)
C_t = Contaminant concentration in the small chamber at time t (mg/m^3)
t = Elapsed time after the start of the test
A = surface area of the specimen (m^2)
Q = Flow rate in small chamber (m^3/h)
n = Number of ventilation (times/h)
V = Volume of small chamber (m^3)
L = Sample load factor (m^2/m^3)
q = Flow rate per unit area (m^3/m^2h)

Emission intensity prediction from building materials

The parameters for the application of the first-order reduction model and the double exponential decay model were calculated as shown in Table 2 below using the initial emission intensity, the first reduction constant, and the second reduction steady of each specimen figured through the small chamber emission experiment, and this was used to predict the emission intensity (Hult et al., 2015; Liang et al., 2016; Seo et al., 2013).

Results

Experimental results and analysis

An important point to be dealt with through this experiment is to identify the characteristics of critical issues that indicate the difference in shape in the graph of the emission pattern (Lim et al., 2014). The variables applied to calculating the predicted value through the empirical model are the initial emission intensity, the maximum emission intensity, and the reduction

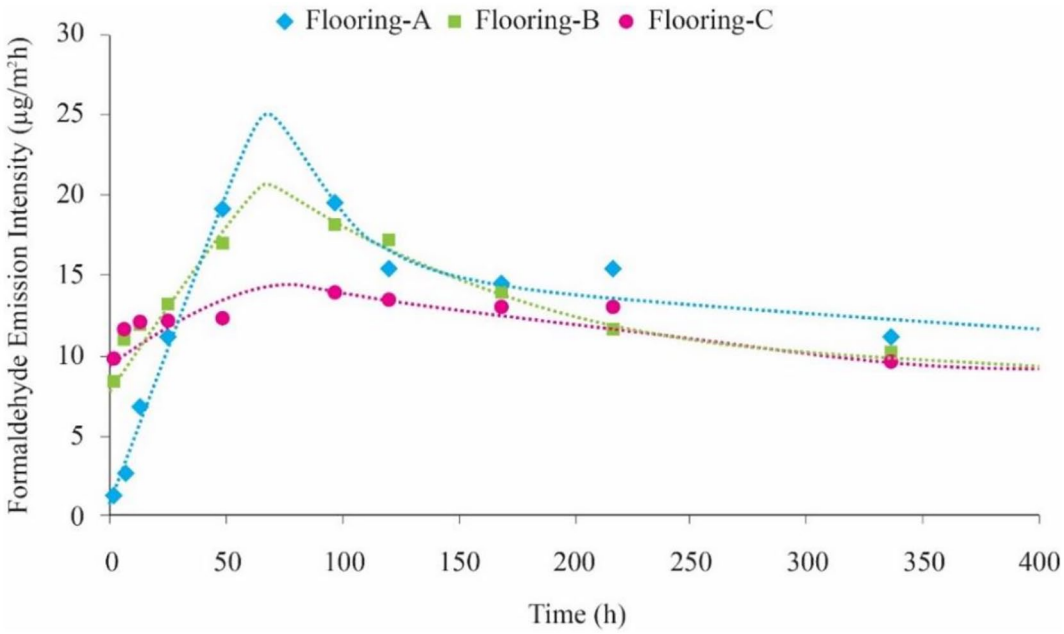

Figure 1. Emission pattern of HCHO over time for each flooring material.

constant (Nogueira et al., 2017). As for the reduction constant, one is applied in the case of a linear reduction model and two in the case of a double exponential decay model (He et al., 2019). In particular, when using the double exponential decay model, it is essential to determine the breakpoint of the change in the descending section (Chi et al., 2016). In the simulation through the empirical model, the researcher has to calculate and input the information of each breakpoint, so the calculation of clear measurement values for these critical points enables valid prediction (Bourdin et al., 2014).

In addition, for each specimen, a concentration change trend line was calculated based on the measurement point to derive an emission pattern. This is based on the dissipation pattern of general building materials, which initially rises for a certain period and then decreases (Liu et al., 2015).

In this section, it is essential to improve the suitability of the predictive model to derive a distinguishing factor by examining the initial emission intensity, which is a crucial point in determining the emission pattern, the shape of the vertex indicating the maximum value, the appearance time of the vertex, and the reduction period that determines the subsequent decrease pattern (Mu et al., 2020). Regression analysis was performed on the fit between the measured and predicted values to analyze the degree of explanation of the linear relationship between predicted and actual values (Shalbafan & Thoemen, 2020).

Analysis and characterization of important breakpoints in emission patterns

Flooring. The initial emission intensity refers to the emission intensity within 24 hours after the specimen is put into a small chamber (An et al., 2010). According to Figure 1, the emission intensity at the first measurement point 1 hour after the material was put into the chamber showed a difference by material. Flooring-A showed the lowest emission intensity at 1.31 μg/m²h but showed a high rate of increase after that. At 24 hours, all materials exhibited emission intensity levels of 11.19 to 13.14 μg/m²h. After that, there is a difference in the form of emission according to the characteristics of each material.

In the case of Flooring-C, it showed the lowest emission intensity within about 100 hours in the initial period. It decreased slightly after that, leading to the lowest cumulative emission amount, as shown in Figure 2. Flooring-A initially showed the lowest emission intensity, increasing rapidly after about 100 hours, offering the highest cumulative emission amount.

It is difficult to predict the degree of emission pattern of alternative materials based on the initial emission intensity alone (Rackes & Waring, 2016). To effectively use the initial emission intensity, it is understood that a pre-treatment process for the experiment after inducing the emission at a temperature close to the experimental temperature for a certain period is necessary (Robertson et al., 2012). Therefore, if the material storage process is not straightforward, conducting the chamber experiment is desirable after undergoing a pre-treatment process for at least 24 hours.

The shape of the graph of the emission pattern changes according to the form of the vertex. It is a significant time because it is usually classified into an increasing section and a decreasing section of chemical substances. As for the shape of the vertices, in the case of Flooring-A and B, the shape of the bell is taken, and in the case of Flooring-C, the form of the vertex is a gentle curve. In this study, flooring-C with relatively low cumulative emission had a soft curve shape, and flooring-A

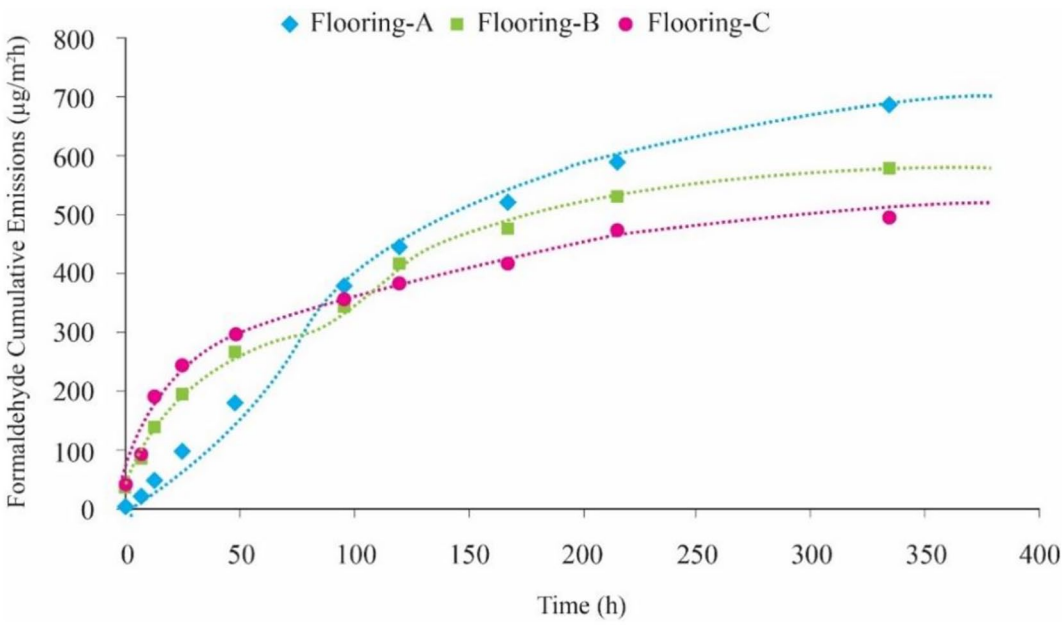

Figure 2. Cumulative emission of HCHO over time for each flooring material.

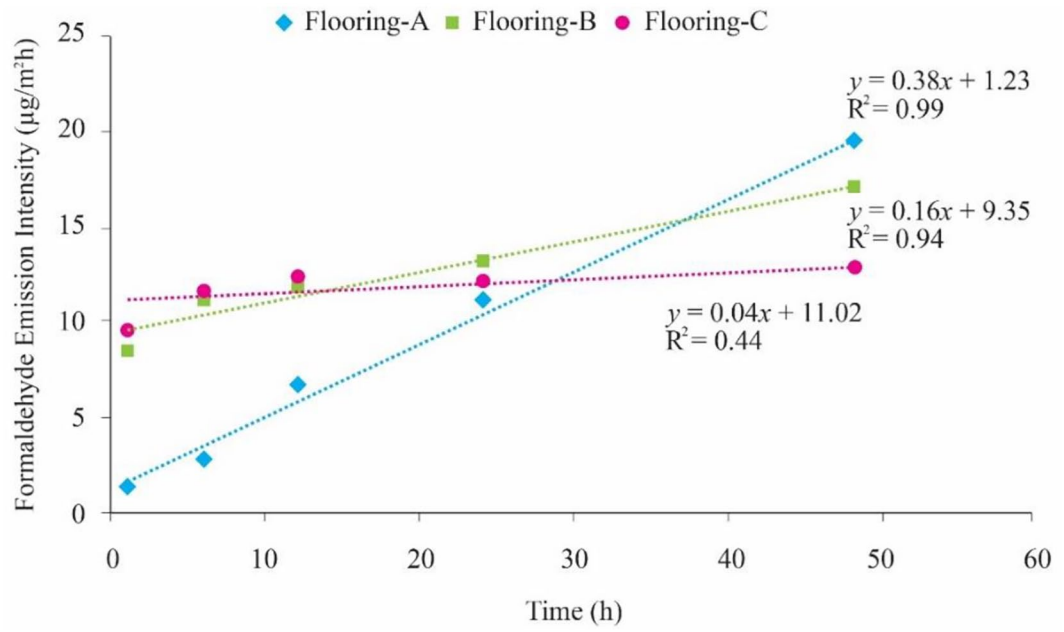

Figure 3. Linear correlation with HCHO in the concentration ascending section for each flooring material.

and B with high cumulative emission showed a bell-shaped vertex. Flooring-A showed the most distinct diffusion pattern of increasing and decreasing concentration.

Figure 3 shows the degree of the linear relationship between the emission intensity and the elapsed time from 1 to 48 hours after material input, based on the vertex of each flooring material. In the case of flooring-A and flooring-B, the bell-shaped vertex was derived, R^2, which indicates the degree of the linear relationship between time elapsed and emission intensity, was .94 or more, showing a solid linear relationship. In the case of flooring-C, R^2 was .44, indicating a relatively low degree of a linear relationship.

The section where the emission intensity decreases from the vertex shows a more complex shape. In applying the empirical model, in the case of the first-order reduction model, it is assumed that the reduction trend decreases linearly in the concentration-falling section. The double exponential decay model is a case where it is considered that this part is divided into two parts, an area in which the decay occurs rapidly and a section in which the reduction occurs slowly. Therefore, looking at the degree of relationship that can infer these linear relationships, in the case of flooring-C, R^2 was .88, and that of flooring-B was .89. Flooring-A showed a slightly weakened linearity of .76.

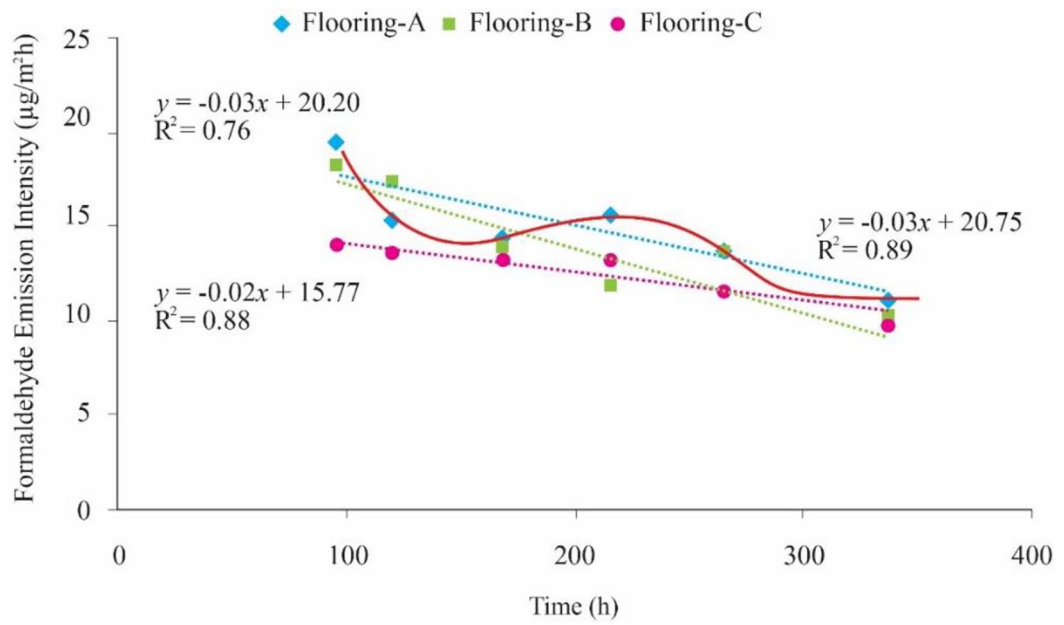

Figure 4. Linear correlation with HCHO in the concentration descending section for each flooring material.

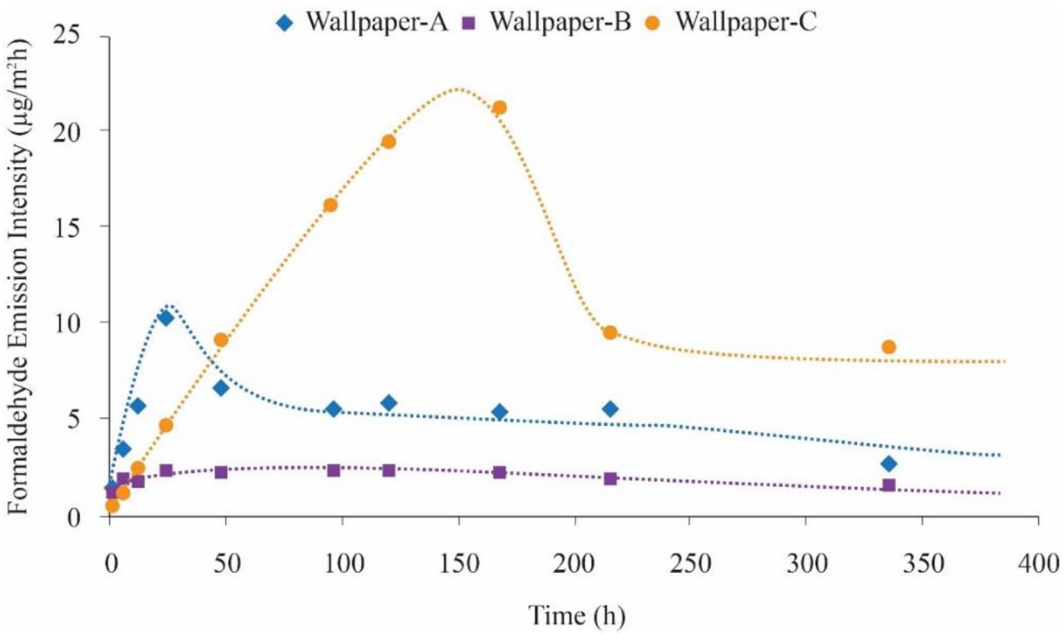

Figure 5. Emission pattern of HCHO over time for each wallpaper.

In the case of flooring-A, which significantly deviates from the linear relationship in the concentration drop section, there are two inflection points in the reduction pattern, as shown in Figure 4. It is judged that the double exponential decay model is more suitable, and it is inferred that the first-order reduction model is more ideal for flooring-C and flooring-B.

Wallpaper. In the case of wallpaper, the initial emission intensity at the time point 1 hour after injecting the sample into the chamber was in the range of 0.75 to 1.48 μg/m²h for each wallpaper, showing a similar level. After 24 hours were completed, the difference in emission intensity for each wallpaper was demonstrated.

As shown in Figure 5. Wallpaper-C exhibited a maximum release intensity of 21.90 μg/m²h at 144 hours, and Wallpaper-A exhibited a maximum release intensity of 10.26 μg/m²h at 24 hours. After the peak, there was a rapid decrease followed by a gradual decrease. Wallpaper-B showed a tendency to slightly increase and decrease without significant change in concentration in almost all sections.

The following is an analysis of the shape of the vertices in the graph of the diffusion pattern. Wallpaper-A showed the highest release intensity when 24 hours had elapsed, and in the case of Wallpaper-C, when 144 hours had elapsed after the sample was added. This corresponds to the vertex of the bell on

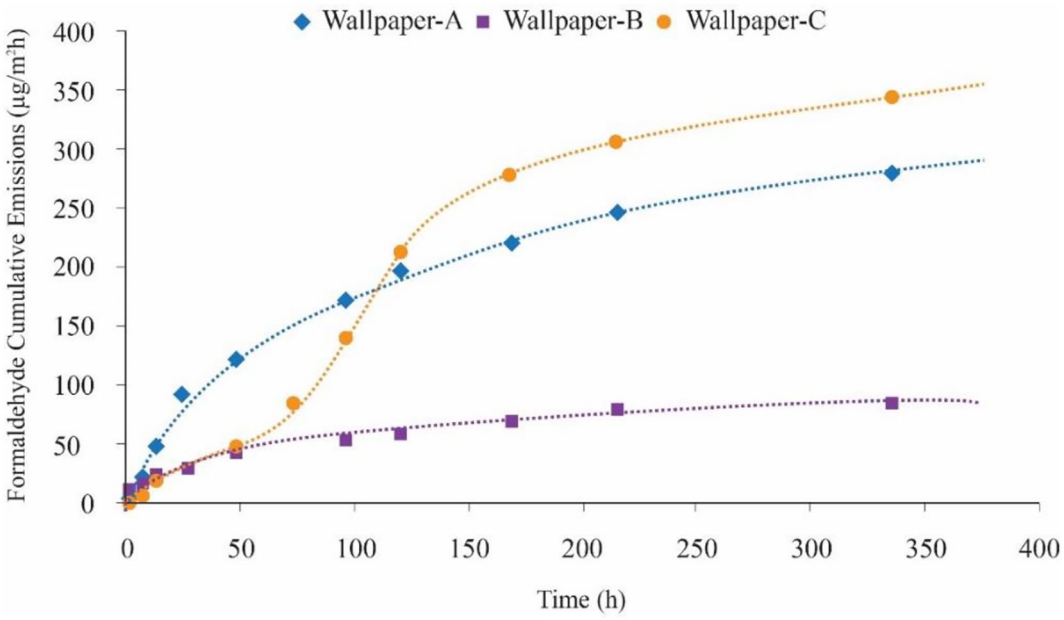

Figure 6. Cumulative emission of HCHO over time for each wallpaper.

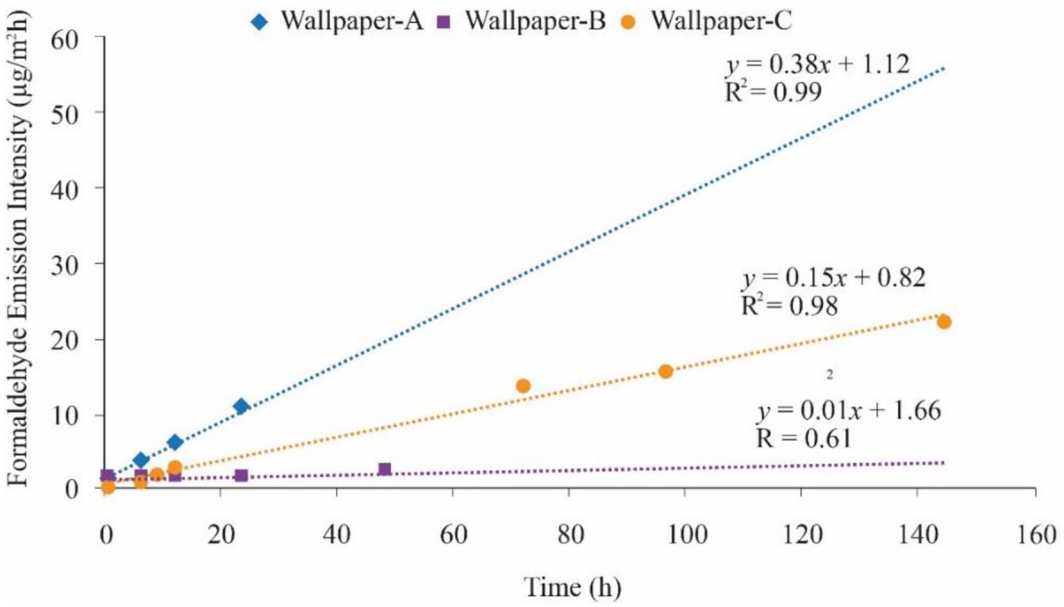

Figure 7. Linear correlation with HCHO in the concentration ascending section for each wallpaper.

the graph. It can be seen that wallpaper-A and wallpaper-C show a difference in the time points representing the peaks of the highest emission intensity. As shown in Figure 6, it can be confirmed that the peak appearance time is delayed in the case of wallpaper-C, which has the most significant cumulative emission. A graph of a typical bell-shaped dissipation pattern showing a continuous decrease after a constant increase is shown. However, in the case of Wallpaper-B, it was confirmed that the diffusion pattern showed a gentle curve rather than a vertex, and the cumulative emission amount was also the least.

As shown in Figure 7, in the linear relationship between the time elapsed to the peak and the emission intensity in the concentration rise section, wallpaper-A and wallpaper-C, which have bell-shaped vertices, have a strong linear relationship with R^2 .98 or more. Wallpaper-B was .61, indicating a weak linear relationship. In addition, in the case of wallpaper-B, R^2 was .91, showing an excellent linear relationship in the concentration decreasing section. In wallpaper-A and wallpaper-C, R^2 was less than .78, indicating a weak linear relationship.

As shown in Figure 8, there is an inflection of the measurement points deviating from the line graph in the case of wallpaper-A and wallpaper-C. In this case, it is judged that applying the double exponential decay model is reasonable. When it has

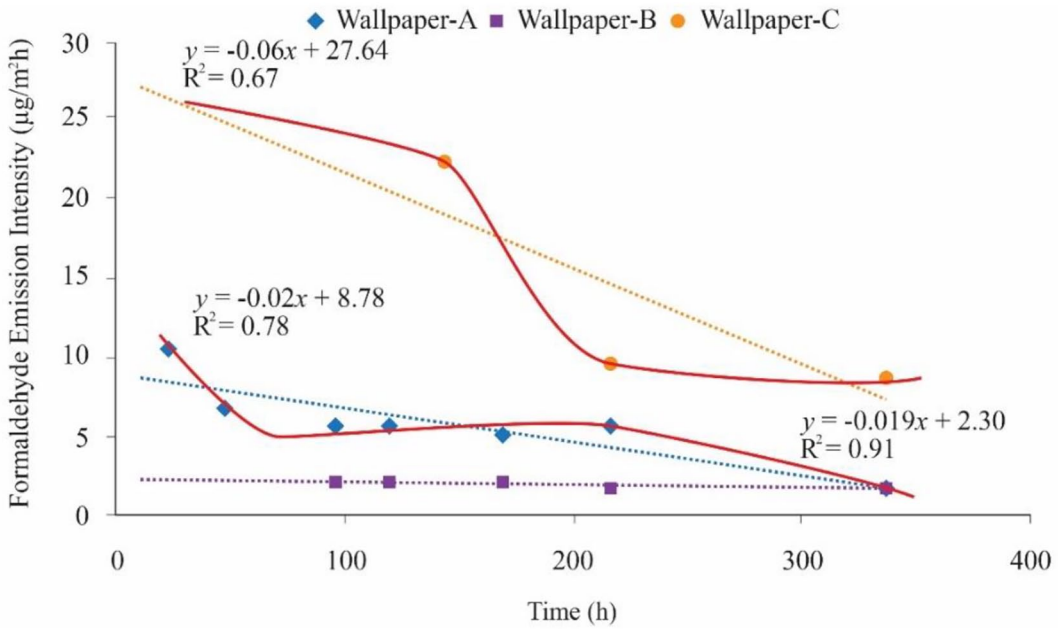

Figure 8. Linear correlation with HCHO in the concentration descending section for each wallpaper.

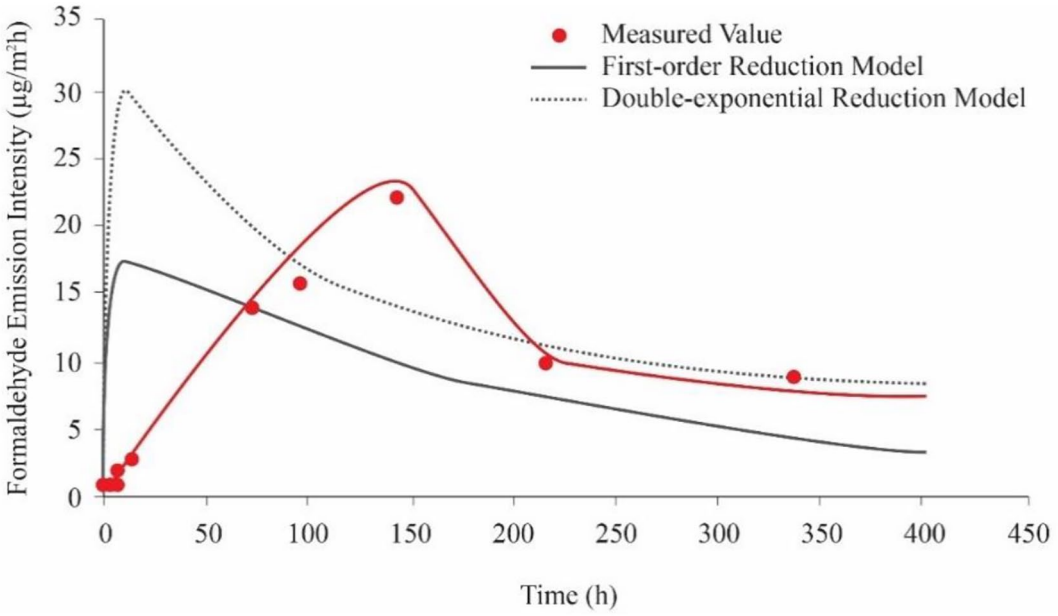

Figure 9. Emission pattern of HCHO based on the measured and predicted values of wallpaper-C.

a bell-shaped vertex in the diffusion pattern and a clear concentration reduction pattern is secured, it is predicted that the double exponential decay model will be helpful, and the first-order reduction model is suitable for showing a strong linear relationship in the concentration reduction section.

Emission intensity prediction result

The emission pattern was classified into three types by comparing the way for each building material obtained in this experiment with the results predicted by each model (Jiang et al., 2017; Zhou et al., 2016). In addition, regression analysis analyzed the fit between the measured and indicated values, and critical points' characteristics were derived for selecting a suitable model for each type (Li et al., 2019).

Type I emission pattern. Type I is an emission pattern that shows a low fit between the measured and predicted values in the entire interval. In particular, it offers a difference between the expected value and the actual value for the peak emission intensity. The measured value has a characteristic that significantly deviates from the prediction pattern of the two models (Frihart et al., 2020). Wallpaper-C, which was shown to have a relatively high HCHO, corresponds to this type.

Figure 9 shows the emission patterns of the predicted and measured values of HCHO using the linear and double

exponential decay models for wallpaper-C. There is a big difference in the emission pattern between the predicted and measured values according to the difference in the time point showing the highest emission intensity.

For this type, as shown in Table 3, R^2, which shows the explanatory power between the predicted values for the measured values of the entire section, was .11 in the first-order reduction model and .00 in the double exponential decay model, indicating no or shallow level of explanatory power.

The explanatory power R^2 of the predicted value in the concentration ascending section was .25 for the first-order reduction model and .19 for the double exponential decay model. This was meaningless at a significant probability of .1 or less. In the concentration descent section, R^2 was .51 in the first-order reduction model and .72 in the double-exponential reduction model, indicating good explanatory power. There was no sign of a significant probability of .1 or less.

Type II Emission pattern. In Type II, the emission pattern of the measured values in the entire section is close to the emission pattern of the predicted values by the two models. Consistency is high in the descending concentration area, and the peak emission intensity appears later than the expected value (Wei et al., 2013). Figure 10 shows the emission pattern of the HCHO predicted value and the actual value predicted using the first-order and double exponential decay models for flooring-A.

As shown in Table 3, R^2, the degree of explanation of the predicted values for the actual values in the entire interval was .00 for the first-order reduction model and .13 for the double exponential decay model.

In addition, in the concentration ascending section based on the vertex, R^2 was found to be .02 for the first-order decay model and .15 for the double exponential decay model.

In the concentration descending section, the first-order decay model was .56, and the double exponential decay model was .72, indicating a relatively good degree of explanation in the concentration descending section. In particular, the explanatory power in the concentration-descent area showed a significant result at a substantial probability of .1 or less. Therefore, in the case of flooring-A, the low suitability of the entire section is pointed out as the cause of the low linear explanatory power in the concentration ascending section.

Wallpaper-A and flooring-B are also divided into the same emission patterns. In the case of wallpaper-A (Figure 11), it can be seen that the emission pattern according to the measured values shows a slight increase in the maximum emission intensity and a gradual decrease in the concentration. According to Table 3, in the case of wallpaper-A, R^2, which shows the explanatory power of the predicted values for the actual values in the entire section, is .41 for the first-order reduction model and .15 for the double exponential decay model. The first-order reduction model showed a relatively higher fit, and in particular, a significant result was established with a substantial probability of .05 or less.

The degree of explanatory value R^2 of the predicted value in the concentration ascending section was .67 for the first-order decay and .70 for the double exponential decay model, but this wasn't very meaningful at a significant probability of .1 or less. On the other hand, in the concentration descending section, the first-order reduction model showed a significant result at the significance level of .05 or less with an R^2 of .72. In the double exponential decay model, R^2 was .53, and the significance probability was less than .05.

The flooring-B (Figure 12) showed relatively low explanatory power in the entire section and was statistically insignificant. R^2 was .23 for the first-order decay model in the concentration ascending section and .20 for the double exponential decay model. These did not show any significant results at a substantial probability of .1 or less.

However, it showed a very high explanatory value in the concentration descending section. In the first-order decay model, R^2 was .92, and in the double exponential decay model, R^2 was .95.

Type II showed extreme suitability in the concentration descending section and a relatively good fit in the ascending section. In addition, it can be seen that the suitability of the predicted values and the actual values for all measurement points improved compared to Type I as the suitability for the concentration ascending section improved.

Type III emission pattern. Type III is an emission pattern that does not show the shape of distinct vertices in the concentration ascending section. It offers a solid linear relationship between the concentration ascending section and the decrease section (Blondel & Plaisance, 2011).

Flooring-C (Figure 13) and wallpaper-B (Figure 14) exhibit an emission pattern that does not have a distinct apex. At the point of declination, the distinction between fast and slow decreases does not occur clearly. Therefore, it is judged that it is unnecessary to distinguish between the first-order decay model and the double exponential reduction model.

As shown in Table 3, in the case of flooring-C, R^2, which indicates the degree of the linear explanatory value of the predicted values for the entire section, was .36 for the first-order decay model and .33 for the double exponential reduction model. This showed a significant result at a substantial probability of .05 or less.

In addition, in the concentration ascending section, R^2 was .93 in both the first-order reduction model and the double-exponential reduction model, indicating a high degree of explanation distinguished from other specimens. This showed a significant result at a substantial probability of .01 or less. An excellent explanatory degree was established in the concentration descending section, and essential development was demonstrated at the significance probability level of .05.

Table 3. Regression Analysis of Measured Values for Each Section and Predicted Values for Each Model.

SECTION			TYPE-I		TYPE-II		TYPE-III	
			WALLPAPER-C	FLOORING-A	FLOORING-B	WALLPAPER-A	FLOORING-C	WALLPAPER-B
Entire section	First-order decay model	R^2	.11 (.641)	.00 (.341)	.17 (.127)	.41 (.027)**	.36 (.040)**	.58 (.006)***
		Equation	$y=-0.26x+11.42$	$y=0.49x+5.21$	$y=0.38x+8.58$	$y=0.73x+1.15$	$y=0.27x+9.20$	$y=0.34x+1.33$
	Double exponential decay model	R^2	.00 (.355)	.13 (.979)	.12 (.177)	.15 (.147)	.33 (.048)**	.60 (.005)***
		Equation	$y=-0.28x+13.72$	$y=11.87x-0.01$	$y=0.21x+9.64$	$y=0.23x+3.25$	$y=0.20x+9.57$	$y=0.25x+1.37$
Concentration ascending section	First-order decay model	R^2	.25 (.991)	.02 (.376)	.23 (.240)	.67 (.117)	.93 (.005)***	.82 (.062)*
		Equation	$y=-0.01x+6.11$	$y=0.61x-0.38$	$y=0.34x+7.61$	$y=0.28x+1.37$	$y=0.22x+0.92$	$y=0.71x+0.48$
	Double exponential decay model	R^2	.19 (.688)	.15 (.542)	.20 (.252)	.70 (.105)	.93 (.005)***	.77 (.079)*
		Equation	$y=-0.15x+9.36$	$y=0.24x+2.05$	$y=0.22x+7.76$	$y=0.21x+1.36$	$y=0.22x+9.24$	$y=0.41x+0.86$
Concentration descending section	First-order decay model	R^2	.51 (.329)	.56 (.089)*	.92 (.007)***	.72 (.021)**	.80 (.027)**	.76 (.013)**
		Equation	$y=2.30x-3.13$	$y=1.08x+1.68$	$y=1.34x-0.93$	$y=0.74x+1.46$	$y=1.07x+0.69$	$y=0.85x+0.47$
	Double exponential decay model	R^2	.72 (.245)	.72 (.043)**	.95 (.005)***	.53 (.062)*	.79 (.028)**	.78 (.013)**
		Equation	$y=2.61x-15.69$	$y=0.58x+5.95$	$y=0.76x+3.25$	$y=0.36x+2.95$	$y=0.61x+4.87$	$y=0.44x+1.04$

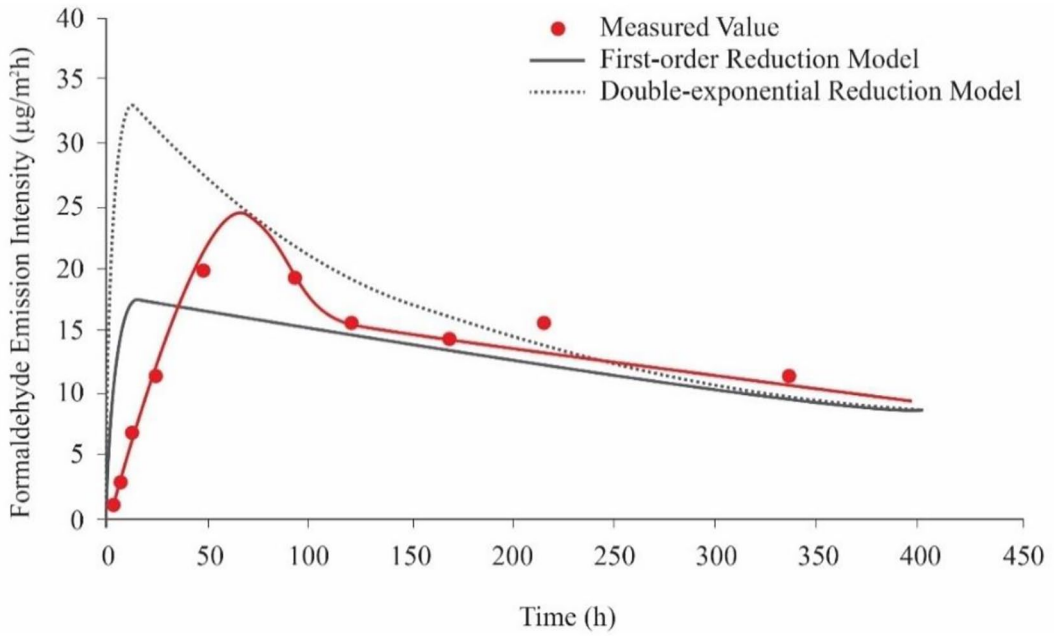

Figure 10. Emission pattern of HCHO based on the measured and predicted values of flooring-A.

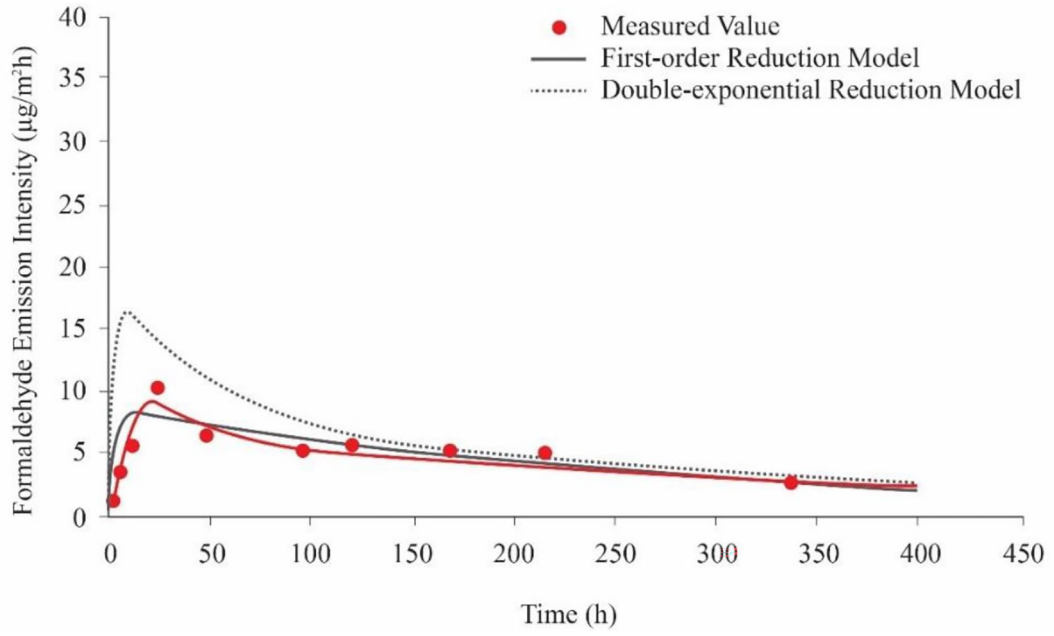

Figure 11. Emission pattern of HCHO based on the measured and predicted values of wallpaper-A.

In wallpaper-B, the first-order decay model had an R^2 of .58 and the double exponential reduction model of .60, indicating a good fit. A significant result was shown with a substantial probability of .01 or less. In addition, the first order and double exponential decay models showed a relatively good fit to the same degree and statistically significant results in the concentration descending section.

In Type III, the explanatory power of the predicted values for the actual values increased in the entire section, and statistically significant results were obtained. In particular, it is judged that the high suitability in the ascending concentration section had a considerable influence.

Discussion

In this study, when the peak appeared late in the emission pattern of HCHO and showed a general characteristic of gently decreasing (Type I and II emission pattern), no significant results were demonstrated in conformity with the predicted values by the empirical model. This is because in the case of building materials with a high content of HCHO, the peak appears later than in the case of the generally expected emission pattern (Salthammer, 2019).

It is judged that it is essential to secure sufficient prediction time for the entire process in the emission pattern in which the appearance of vertices is relatively late (D'Amico et al., 2020). In

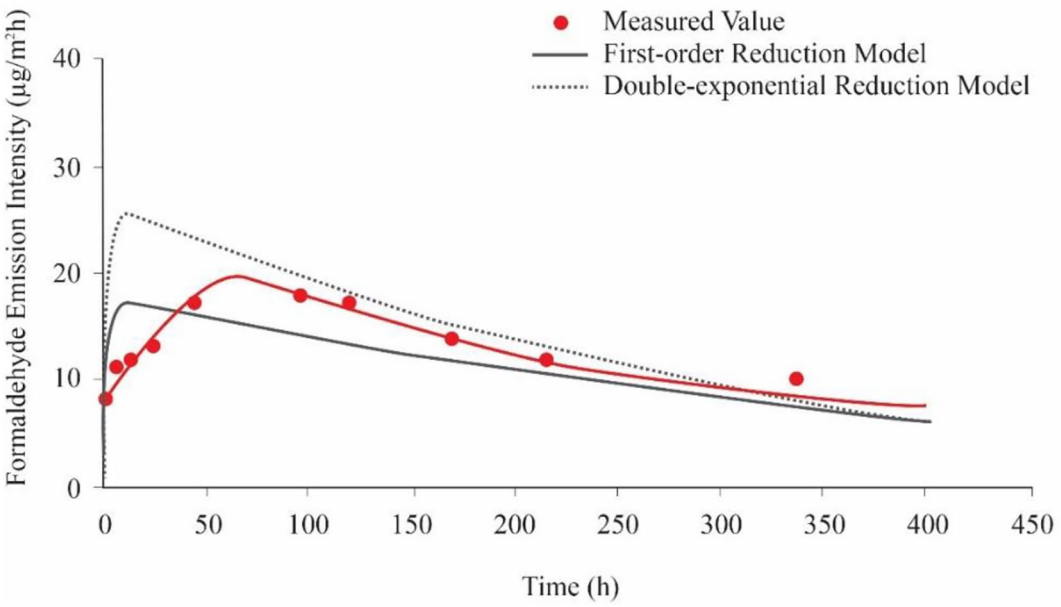

Figure 12. Emission pattern of HCHO based on the measured and predicted values of flooring-B.

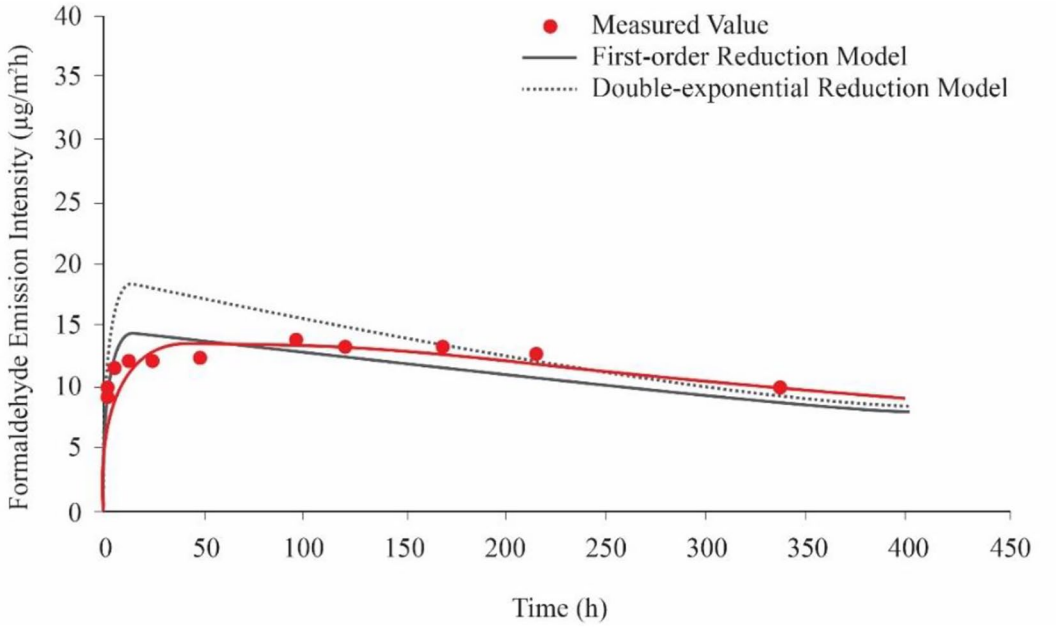

Figure 13. Emission pattern of HCHO based on the measured and predicted values of flooring-C.

the case of the emission pattern of HCHO, it was confirmed that it is a prerequisite for applying the empirical model to secure a sufficient period of reduction after the peak and to position the ultra-high rise early in the total prediction time ratio.

Accordingly, it is necessary to investigate the characteristics of the emission pattern according to the level of HCHO and determine how much time is needed to obtain an appropriate prediction time through further research.

Conclusions

In this study, when an empirical model is applied based on the emission pattern of HCHO for six building material specimens, the effect of each emission pattern on important division points is identified.

1. The judgment for selecting the first-order decay model and the double exponential decay model was based on the fact that the HCHO emission pattern had the shape of a vertex. In addition, the linear relationship between emission intensity and time elapsed in the ascending concentration section was more significant. In the concentration descending area, the linear relationship was weakened. Thus, applying the double exponential decay model was appropriate for two or more inflection point

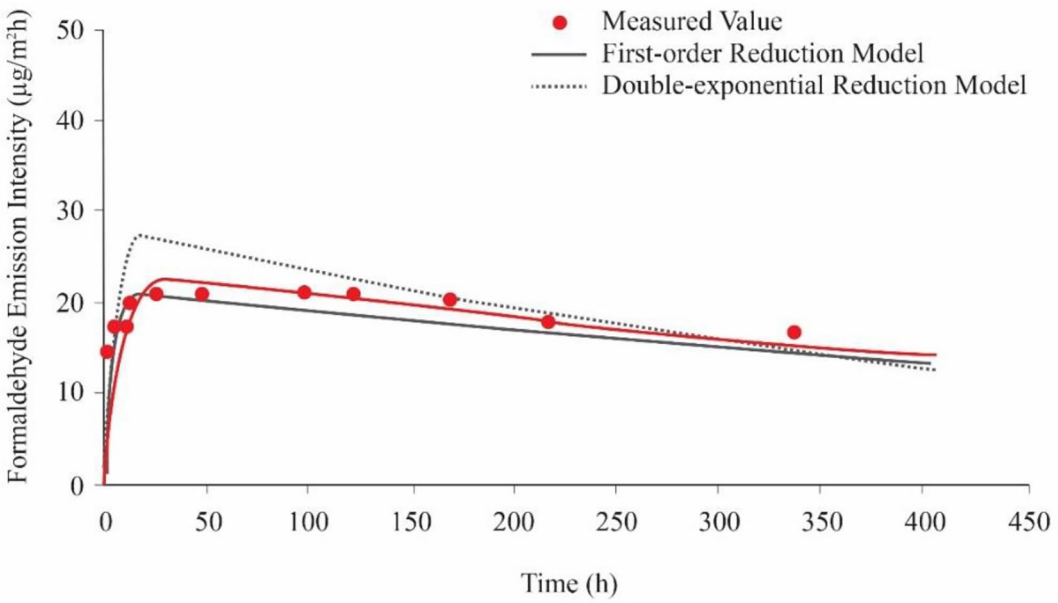

Figure 14. Emission pattern of HCHO based on the measured and predicted values of wallpaper-B.

graphs. When there is a high linear relationship between emission intensity and time elapse in the concentration ascending section and the concentration descending section, it was confirmed that selecting the first-order reduction model was more appropriate.

2. Based on the emission pattern of HCHO in building materials, it was classified into three types according to the characteristics of the compatibility between the predicted values and the actual values. In Type I (R^2 = .02–.25), the emission of chemical substances reaches the maximum after the start of the experiment and decreases relatively rapidly. Type II (R^2 = .67–.70) is an emission pattern with a vertex shape with a slight concentration increase and a gentle decrease. It is a type in which the suitability is significantly high in the concentration descending section. Type III (R^2 = .77–.93) is an emission pattern that shows a mild linear increase and decreases trend in the concentration ascending section and the descending concentration area. It is a type that offers the suitability with the predicted value in a meaningful way in the entire section.
3. Most previous studies decided to apply the first order or double exponential decay model to consider the chemical emission characteristics in the concentration descending section according to the difference in material types. However, this study confirmed that the emission characteristics in the initial concentration ascending section and the concentration descending section are important division points for model selection. This study found that R^2, the degree of explanation of the predicted values for the measured values in the concentration descending section, was in the range of .51 to .95 in all cases and showed a good fit. However, the ascending concentration section distinguished the difference between high and low suitability. Therefore, the suitability of the measured values and the predicted values in the emission pattern of the entire area was most affected by the suitability in the concentration ascending period, so the excellent suitability in the concentration ascending section generally showed suitable suitability in the overall emission pattern.

Acknowledgements

The authors would like to express their gratitude to Ajman University for APC support and Healthy and Sustainable Buildings Research Center at Ajman University for providing great research environment.

Author Contributions

Chuloh Jung: Writing - Original Draft, Conceptualization, Methodology, Data curation.
Naglaa Sami Abdelaziz Mahmoud: Writing—Review & Editing, Investigation, Project Administration, Resources, Software, Formal analysis, Validation, Supervision.

Author Contributions

All authors contributed significantly to this study. C.J. and N.A. identified and secured the example buildings used in the study. The data acquisition system and installation of sensors were designed and installed by C.J. and N.A. N.A. was responsible for data collection. C.J. performed data analysis. The manuscript was compiled by C.J. and reviewed by N.A. All authors have read and agreed to the published version of the manuscript.

Declaration of Conflicting Interests

The author(s) declared no potential conflicts of interest with respect to the research, authorship, and/or publication of this article.

Funding

The author(s) received no financial support for the research, authorship, and/or publication of this article.

ORCID iD

Chuloh Jung https://orcid.org/0000-0002-0898-8450

Data Availability Statement

New data were created or analyzed in this study. Data will be shared upon request and consideration of the authors.

REFERENCES

Ahn, J., Shin, D., Kim, K., & Yang, J. (2017). Indoor air quality analysis using deep learning with sensor data. *Sensors*, 17(11), 2476.

Ai, Z. T., Mak, C. M., & Cui, D. J. (2015). On-site measurements of ventilation performance and indoor air quality in naturally ventilated high-rise residential buildings in Hong Kong. *Indoor and Built Environment*, 24(2), 214–224.

An, J. Y., Kim, S., Kim, H. J., & Seo, J. (2010). Emission behavior of formaldehyde and TVOC from engineered flooring in under heating and air circulation systems. *Building and Environment*, 45(8), 1826–1833.

Arar, M., & Jung, C. (2021). Improving the indoor air quality in nursery buildings in United Arab Emirates. *International Journal of Environmental Research and Public Health*, 18(22), 12091.

Awad, J., & Jung, C. (2021). Evaluating the indoor air quality after renovation at the Greens in Dubai, United Arab Emirates. *Buildings*, 11(8), 353.

Blondel, A., & Plaisance, H. (2011). Screening of formaldehyde indoor sources and quantification of their emission using a passive sampler. *Building and Environment*, 46(6), 1284–1291.

Böhm, M., Salem, M. Z., & Srba, J. (2012). Formaldehyde emission monitoring from a variety of solid wood, plywood, blockboard and flooring products manufactured for building and furnishing materials. *Journal of Hazardous Materials*, *221-222*, 68–79.

Bourdin, D., Mocho, P., Desauziers, V., & Plaisance, H. (2014). Formaldehyde emission behavior of building materials: On-site measurements and modeling approach to predict indoor air pollution. *Journal of Hazardous Materials*, 280, 164–173.

Breen, M. S., Burke, J. M., Batterman, S. A., Vette, A. F., Godwin, C., Croghan, C. W., Schultz, B. D., & Long, T. C. (2014). Modeling spatial and temporal variability of residential air exchange rates for the Near-Road Exposures and Effects of Urban Air Pollutants Study (NEXUS). *International Journal of Environmental Research and Public Health*, 11(11), 11481–11504.

Chi, C., Chen, W., Guo, M., Weng, M., Yan, G., & Shen, X. (2016). Law and features of TVOC and Formaldehyde pollution in urban indoor air. *Atmospheric Environment*, 132, 85–90.

Cho, H. S., & Choi, M. (2014). Effects of compact urban development on air pollution: Empirical evidence from Korea. *Sustainability*, 6(9), 5968–5982.

de Gennaro, G., Loiotile, A. D., Fracchiolla, R., Palmisani, J., Saracino, M. R., & Tutino, M. (2015). Temporal variation of VOC emission from solvent and water based wood stains. *Atmospheric Environment*, 115, 53–61.

D'Amico, A., Bergonzoni, G., Pini, A., & Currà, E. (2020). BIM for healthy buildings: An Integrated approach of architectural design based on IAQ_prediction. *Sustainability*, 12(24), 10417.

D'Ovidio, M. C., Di Renzi, S., Capone, P., & Pelliccioni, A. (2021). Pollen and fungal spores evaluation in relation to occupants and microclimate in indoor workplaces. *Sustainability*, 13(6), 3154.

Even, M., Wilke, O., Kalus, S., Schultes, P., Hutzler, C., & Luch, A. (2021). Formaldehyde emissions from wooden toys: Comparison of different measurement methods and assessment of exposure. *Materials*, 14(2), 262.

Frihart, C. R., Chaffee, T. L., & Wescott, J. M. (2020). Long-term formaldehyde emission potential from UF- and NAF-bonded particleboards. *Polymers*, 12(8), 1852.

Geng, Y., Ji, W., Lin, B., & Zhu, Y. (2017). The impact of thermal environment on occupant IEQ_perception and productivity. *Building and Environment*, 121, 158–167.

Gunschera, J., Mentese, S., Salthammer, T., & Andersen, J. R. (2013). Impact of building materials on indoor formaldehyde levels: Effect of ceiling tiles, mineral fiber insulation and gypsum board. *Building and Environment*, 64, 138–145.

Gładyszewska-Fiedoruk, K., Zhelykh, V., & Pushchinskyi, A. (2019). Simulation and analysis of various ventilation systems given in an example in the same school of indoor air quality. *Energies*, 12(15), 2845.

Hérault, B., Beauchêne, J., Muller, F., Wagner, F., Baraloto, C., Blanc, L., & Martin, J. M. (2010). Modeling decay rates of dead wood in a neotropical forest. *Oecologia*, 164(1), 243–251.

He, Z., Xiong, J., Kumagai, K., & Chen, W. (2019). An improved mechanism-based model for predicting the long-term formaldehyde emissions from composite wood products with exposed edges and seams. *Environment International*, 132, 105086.

Huang, Y., Ho, S. S., Lu, Y., Niu, R., Xu, L., Cao, J., & Lee, S. (2016). Removal of indoor volatile organic compounds via photocatalytic oxidation: A short review and prospect. *Molecules*, 21(1), 56.

Hult, E. L., Willem, H., Price, P. N., Hotchi, T., Russell, M. L., & Singer, B. C. (2015). Formaldehyde and acetaldehyde exposure mitigation in US residences: In-home measurements of ventilation control and source control. *Indoor Air*, 25(5), 523–535.

ISO. (2020). Indoor air — Part 28: Determination of odour emissions from building products using test chambers. https://www.iso.org/obp/ui/#iso:std:iso:16000:-28:ed-2:v1:en

Jiang, C., Li, D., Zhang, P., Li, J., Wang, J., & Yu, J. (2017). Formaldehyde and volatile organic compound (VOC) emissions from particleboard: Identification of odorous compounds and effects of heat treatment. *Building and Environment*, 117, 118–126.

Jomehzadeh, F., Nejat, P., Calautit, J. K., Yusof, M. B. M., Zaki, S. A., Hughes, B. R., & Yazid, M. N. A. W. M. (2017). A review on windcatcher for passive cooling and natural ventilation in buildings, Part 1: Indoor air quality and thermal comfort assessment. *Renewable and Sustainable Energy Reviews*, 70, 736–756.

Jung, C., & Awad, J. (2021). The improvement of indoor air quality in residential buildings in Dubai, UAE. *Buildings*, 11(6), 250.

Jung, C., Awad, J., Sami Abdelaziz Mahmoud, N., & Salameh, M. (2021). An analysis of indoor environment evaluation for the Springs development in Dubai, UAE. *Open House International*, 46, 651–667.

Khoshnava, S. M., Rostami, R., Mohamad Zin, R., Štreimikienė, D., Mardani, A., & Ismail, M. (2020). The role of green building materials in reducing environmental and human health impacts. *International Journal of Environmental Research and Public Health*, 17(7), 2589.

Kozicki, M., & Guzik, K. (2021). Comparison of VOC emissions produced by different types of adhesives based on test chambers. *Materials*, 14(8), 1924.

Kubečková, D., Kraus, M., Šenitková, I. J., & Vrbová, M. (2020). The indoor microclimate of prefabricated buildings for housing: Interaction of environmental and construction measures. *Sustainability*, 12(23), 10119.

Liang, W., Lv, M., & Yang, X. (2016). The effect of humidity on formaldehyde emission parameters of a medium-density fiberboard: Experimental observations and correlations. *Building and Environment*, 101, 110–115.

Liang, W., & Yang, X. (2013). Indoor formaldehyde in real buildings: Emission source identification, overall emission rate estimation, concentration increase and decay patterns. *Building and Environment*, 69, 114–120.

Lim, J., Kim, S., Kim, A., Lee, W., Han, J., & Cha, J. S. (2014). Behavior of VOCs and carbonyl compounds emission from different types of wallpapers in Korea. *International Journal of Environmental Research and Public Health*, 11(4), 4326–4339.

Liu, X., Mason, M. A., Guo, Z., Krebs, K. A., & Roache, N. F. (2015). Source emission and model evaluation of formaldehyde from composite and solid wood furniture in a full-scale chamber. *Atmospheric Environment*, 122, 561–568.

Li, X., Gao, Q., Xia, C., Li, J., & Zhou, X. (2019). Urea formaldehyde resin resultant plywood with rapid formaldehyde release modified by tunnel-structured sepiolite. *Polymers*, 11(8), 1286.

Marzocca, A., Di Gilio, A., Farella, G., Giua, R., & de Gennaro, G. (2017). Indoor air quality assessment and study of different VOC contributions within a school in Taranto City, South of Italy. *Environments*, 4(1), 23.

Missia, D. A., Demetriou, E., Michael, N., Tolis, E. I., & Bartzis, J. G. (2010). Indoor exposure from building materials: A field study. *Atmospheric Environment*, 44(35), 4388–4395.

Mocho, P., Desauziers, V., Plaisance, H., & Sauvat, N. (2017). Improvement of the performance of a simple box model using CFD modeling to predict indoor air formaldehyde concentration. *Building and Environment*, 124, 450–459.

Murata, K., Watanabe, Y., & Nakano, T. (2013). Effect of thermal treatment of veneer on formaldehyde emission of poplar plywood. *Materials*, 6(2), 410–420.

Mu, Y. T., Li, Z. A., Gu, Z. L., & Tao, W. Q. (2020). Computational fluid dynamics prediction of formaldehyde emission and sorption processes in a small test chamber with mixing fan and vents. *Atmospheric Environment*, 229, 117455.

Nogueira, T., Dominutti, P., Fornaro, A., & Andrade, M. (2017). Seasonal trends of formaldehyde and acetaldehyde in the megacity of São Paulo. *Atmosphere*, 8(8), 144.

Palmisani, J., Di Gilio, A., Cisternino, E., Tutino, M., & de Gennaro, G. (2020). Volatile Organic Compound (VOC) emissions from a personal care polymer-based item: Simulation of the inhalation exposure scenario indoors under actual conditions of use. *Sustainability*, 12(7), 2577.

Peng, Z., Deng, W., & Tenorio, R. (2017). Investigation of indoor air quality and the identification of influential factors at primary schools in the North of China. *Sustainability*, 9(7), 1180.

Piasecki, M., & Kostyrko, K. (2020). Development of weighting scheme for indoor air quality model using a multi-attribute decision making method. *Energies*, 13(12), 3120.

Piasecki, M., Kozicki, M., Firląg, S., Goljan, A., & Kostyrko, K. (2018). The approach of including TVOCs concentration in the indoor environmental quality model (IEQ)—Case studies of BREEAM certified office buildings. *Sustainability*, 10(11), 3902.

Rackes, A., & Waring, M. S. (2016). Do time-averaged, whole-building, effective volatile organic compound (VOC) emissions depend on the air exchange rate? A statistical analysis of trends for 46 VOC s in US offices. *Indoor Air*, 26(4), 642–659.

Robertson, A. B., Lam, F. C. F., & Cole, R. J. (2012). A comparative cradle-to-gate life cycle assessment of mid-rise office building construction alternatives: Laminated timber or reinforced concrete. *Buildings*, 2(3), 245–270.

Rosen, M. A., & Kishawy, H. A. (2012). Sustainable manufacturing and design: Concepts, practices and needs. *Sustainability*, 4(2), 154–174.

Salem, M. Z. M., Böhm, M., Srba, J., & Beránková, J. (2012). Evaluation of formaldehyde emission from different types of wood-based panels and flooring materials using different standard test methods. *Building and Environment*, 49, 86–96.

Salthammer, T. (2019). Formaldehyde sources, formaldehyde concentrations and air exchange rates in European housings. *Building and Environment*, 150, 219–232.

Sarbu, I., & Sebarchievici, C. (2013). Aspects of indoor environmental quality assessment in buildings. *Energy and Buildings*, 60, 410–419.

Seo, J., Ataka, Y., Kato, S., & Kim, J. T. (2013). Long/short-term performance test for evaluating the reduction of indoor formaldehyde using sorptive building materials. *Indoor and Built Environment*, 22(1), 52–60.

Shalbafan, A., & Thoemen, H. (2020). Geopolymer-bonded laminated veneer lumber as environmentally friendly and formaldehyde-free product: Effect of various additives on geopolymer binder features. *Applied Sciences*, 10(2), 593.

Tran, V. V., Park, D., & Lee, Y. C. (2020). Indoor air pollution, related human diseases, and recent trends in the control and improvement of indoor air quality. *International Journal of Environmental Research and Public Health*, 17(8), 2927.

Tucker, S. P. (2014). Development, evaluation and comparison of two independent sampling and analytical methods for ortho-phthalaldehyde vapors and condensation aerosols in air. *Analytical Methods*, 6(8), 2592–2607.

Tudor, E. M., Barbu, M. C., Petutschnigg, A., Réh, R., & Krišťák. (2020). Analysis of larch-bark capacity for formaldehyde removal in wood adhesives. *International Journal of Environmental Research and Public Health*, 17(3), 764.

Wang, X., Hong, S., Lian, H., Zhan, X., Cheng, M., Huang, Z., Manzo, M., Cai, L., Nadda, A., Le, Q. V., & Xia, C. (2021). Photocatalytic degradation of surface-coated tourmaline-titanium dioxide for self-cleaning of formaldehyde emitted from furniture. *Journal of Hazardous Materials*, 420, 126565.

Wei, W., Howard-Reed, C., Persily, A., & Zhang, Y. (2013). Standard formaldehyde source for chamber testing of material emissions: Model development, experimental evaluation, and impacts of environmental factors. *Environmental Science & Technology*, 47(14), 7848–7854.

Williams, J., Li, H., Ross, A. B., & Hargreaves, S. P. (2019). Quantification of the influence of NO2, NO and CO gases on the determination of formaldehyde and acetaldehyde using the DNPH method as applied to polluted environments. *Atmospheric Environment*, 218, 117019.

Wi, S., Kim, M. G., Myung, S. W., Baik, Y. K., Lee, K. B., Song, H. S., Kwak, M. J., & Kim, S. (2020). Evaluation and analysis of volatile organic compounds and formaldehyde emission of building products in accordance with legal standards: A statistical experimental study. *Journal of Hazardous Materials*, 393, 122381.

Xing, J., Li, S., Ding, D., Kelly, J. T., Wang, S., Jang, C., Zhu, Y., & Hao, J. (2020). Data assimilation of ambient concentrations of multiple air pollutants using an emission-concentration response modeling framework. *Atmosphere*, 11(12), 1289.

Xiong, J., Chen, F., Sun, L., Yu, X., Zhao, J., Hu, Y., & Wang, Y. (2019). Characterization of VOC emissions from composite wood furniture: Parameter determination and simplified model. *Building and Environment*, 161, 106237.

Zhang, J., Sun, R., Chen, Y., Tan, K., Wei, H., Yin, L., & Pu, Y. (2014). Small molecule metabolite biomarker candidates in urine from mice exposed to formaldehyde. *International Journal of Molecular Sciences*, 15(9), 16458–16468.

Zhou, X., Liu, Y., Song, C., & Liu, J. (2016). A study on the formaldehyde emission parameters of porous building materials based on adsorption potential theory. *Building and Environment*, 106, 254–264.